Development 136, 2997-3006 (2009) doi:10.1242/dev.033811

Auxin patterns *Solanum lycopersicum* leaf morphogenesis

Daniel Koenig[1], Emmanuelle Bayer[2], Julie Kang[1], Cris Kuhlemeier[2] and Neelima Sinha[1,*]

One of the most striking aspects of plant diversity is variation in leaf shape. Much of this diversity is achieved by the modulation of leaf blade dissection to form lobes or leaflets. Here, we show that the phytohormone auxin is a crucial signal regulating the partitioned outgrowth necessary to develop a dissected leaf. In developing leaves, the asymmetric distribution of auxin, driven by active transport, delineates the initiation of lobes and leaflets and specifies differential laminar outgrowth. Furthermore, homologous members of the AUX/indole-3-acetic acid (IAA) gene family mediate the action of auxin in determining leaf shape by repressing outgrowth in areas of low auxin concentration during both simple and compound leaf development. These results provide molecular evidence that leaflets initiate in a process reminiscent of organogenesis at the shoot apical meristem, but that compound and simple leaves regulate marginal growth through an evolutionarily conserved mechanism, thus shedding light on the homology of compound and simple leaves.

KEY WORDS: Auxin, Leaf morphology, Compound leaf, Dissected leaf, Leaflet, ENTIRE, PIN1, Tomato

INTRODUCTION

The lateral organs of flowering plants show a tremendous diversity in shape and size that has long fascinated both scientists and botanical enthusiasts. Plant leaves are no exception to this phenomenon, despite a broadly conserved role in photosynthetic light capture. Leaf morphology is divided into two major types: simple leaves consisting of a single continuous blade; and compound leaves consisting of multiple discontinuous blade units termed leaflets. Simple and compound leaf morphology is further subdivided into lobed and unlobed types. Despite a long-standing interest in the basis of morphological diversity, the molecular mechanisms that give rise to variation in leaf shape are incompletely understood.

Recent studies have found that genes that regulate indeterminacy at the shoot apical meristem (SAM) (Long et al., 1996; Vollbrecht et al., 2000; Vollbrecht et al., 1990), such as the KNOTTED-LIKE HOMEOBOX (KNOX) genes, are important regulators of compound leaf development (Bharathan et al., 2002; Brand et al., 2007; Hay and Tsiantis, 2006). The expansion of KNOX gene expression in compound-leafed species into the leaf primordia appears to be necessary to promote leaflet initiation. Interestingly, the expression of KNOX genes is also found in the developing leaves of many simple-leafed species (Bharathan et al., 2002). These simple-leafed species morphologically resemble compound-leafed species during early leaf development, but subsequent differential blade outgrowth results in a simple leaf. These data confirm classical studies that separated leaf development into two phases: primary morphogenesis, in which leaflets are initiated; and secondary morphogenesis, in which the pattern of blade outgrowth is determined (Hagemann and Glesissberg, 1996). KNOX gene expression in leaves is not sufficient to promote leaf dissection during secondary morphogenesis (Bharathan et al., 2002), suggesting that other factors regulate differential growth during this stage of leaf development.

[1]Section of Plant Biology, University of California, One Shields Avenue, Davis, CA 95616, USA. [2]Institute of Plant Sciences, University of Bern, Altenbergrain 21, CH-3013 Bern, Switzerland.

*Author for correspondence (nrsinha@ucdavis.edu)

Accepted 26 June 2009

In *Arabidopsis thaliana*, the plant hormone auxin has been implicated as a signal in the pattern of organ initiation from the SAM, the development of leaf serrations and the generation of leaf vascular tissue (Benkova et al., 2003; Hay et al., 2006; Reinhardt et al., 2000; Reinhardt et al., 2003; Scarpella et al., 2006). The active transport of auxin by the PIN-FORMED (PIN) family of auxin efflux carriers plays a major role in the development of auxin maxima that pattern all of these events (Benkova et al., 2003; Hay et al., 2006; Heisler et al., 2005; Petrasek et al., 2006; Scarpella et al., 2006). *pin1* loss-of-function mutants fail to initiate reproductive lateral organs and produce leaves with altered vascular tissue patterning (Galweiler et al., 1998; Koizumi et al., 2005; Mattsson et al., 1999; Okada et al., 1991). PIN1 directs auxin efflux via polar subcellular localization, and the convergence of PIN1 localization in the epidermis is associated with auxin maxima that delineate the downstream initiation of leaf primordia, leaf serrations or leaf vascular tissue (Bayer et al., 2009; Benkova et al., 2003; Hay et al., 2006; Scarpella et al., 2006). PIN1 expression itself is upregulated by auxin, possibly resulting in an amplification of the auxin maximum (Bayer et al., 2009; Heisler et al., 2005). The conserved role of auxin in the specification of developmental pattern, and the resemblance between leaf and leaflet initiation, makes auxin an excellent candidate as a regulator of the morphological patterning of compound leaves.

Recently, a number of studies have implicated auxin distribution as a patterning mechanism during compound leaf development. Chemical disruption of auxin transport results in leaf simplification (Avasarala et al., 1996; Barkoulas et al., 2008; DeMason and Chawla, 2004; Reinhardt et al., 2000) and *pin1* mutants in the compound-leafed species *Cardamine hirsuta* produce simple leaves (Barkoulas et al., 2008). *Ch*PIN1 localization after leaflet initiation closely resembles the reported PIN1 localization subsequent to leaf initiation in *A. thaliana*. Moreover, activation of the response to auxin precedes leaflet outgrowth in *C. hirsuta* leaves, and is observed in initiated leaflets in pea (DeMason and Polowick, 2009). Whole-plant treatment of *C. hirsuta* with exogenous auxin is sufficient to induce ectopic growth along the leaf rachis, suggesting that auxin controls blade outgrowth in leaves. Finally, the simple-leafed tomato mutant *entire* results from loss of function of the auxin response component *LeIAA9* (Wang et al., 2005; Zhang et al., 2007). Together, these results strongly implicate auxin and the response to auxin in the development of compound leaves.

These independent studies in pea, *A. thaliana*, *C. hirsuta* and tomato make it difficult to integrate the roles of various components in leaf shape regulation. It is also not clear what the exact function of auxin is during the primary and secondary morphogenesis stages of leaf development. Controlled local application of auxin to developing leaves is necessary to discern the direct relationship between hormone application and morphological outcome. Finally, although compound leaf development has evolved independently many times, PIN1 localization has been observed in detail during leaf development in a single compound-leafed species. Thus, it is of interest to determine whether convergent evolution of the compound leaf trait utilizes the PIN/auxin developmental module in a similar manner. To address these issues we have investigated the role of auxin and the response to auxin during tomato compound leaf development. Tomato represents an independent origin of compound leaves separated by over 100 million years from that of *C. hirsuta* and pea. We find that auxin regulates both the initiation of leaflets during primary morphogenesis and blade outgrowth during secondary morphogenesis in tomato. This second process is mediated by *ENTIRE*, and homologous AUX/IAA genes modulate marginal growth in the simple leaves of *A. thaliana*. These results provide a molecular and physiological framework for understanding how dissected leaf shape is produced.

MATERIALS AND METHODS

Plant material and growth conditions

Tomato seeds (LA2838A, LA2706 and LA2922) were obtained from the Tomato Genetics Resource Center (TGRC). Tomatoes were germinated in soil, grown in growth chambers at 22°C and under 24-hour days. The *Arabidopsis thaliana* genotypes (CS25210, CS25211 and CS25223) were ordered from the *Arabidopsis* Biological Resource Center (ARBC). *A. thaliana* was grown under 24-hour light conditions at 21°C.

Plant tissue culture and auxin application experiments

Shoots were cultured as previously described (Fleming et al., 1999). For NPA treatment, shoots were allowed to grow on control or 10 μm NPA media for 4 to 7 days and then visualized. Auxin applications (1 mM or 10 mM IAA, or 1% DMSO as a control) were performed as previously conducted in SAMs (Reinhardt et al., 2000) on P2- and P3-staged leaves. Shoots were then allowed to grow in culture for 4 days before visualization. For mature leaf morphology, shoots were transferred to soil and maintained in high humidity. Recovered shoots then grew for several weeks until leaves were large enough for imaging. Moneymaker, VF36 and Ailsa Craig tomato varieties were used as wild type in these experiments.

Histology and immunochemistry

PIN1 immunolocalizations were performed as previously described (Bayer et al., 2009). The *ENTIRE* RNA in situ hybridization was carried out as described in Garces et al. (Garces et al., 2007), with minor modifications. Sense and antisense *ENTIRE* probe templates were generated by PCR amplification from a cDNA template using primers IAA9-F5 (5′-GGTTCCCACAGGATTATTAGAGTG-3′) and IAA9-R2 (5′-ACTTC-CCCTCTGAGAATCC-3′), and cloning into the pCR2.1 vector using the TOPO TA Cloning Kit (Invitrogen, Carlsbad, CA, USA). Images from both immunolocalization and in situ hybridization experiments are representative of data acquired from over ten apices in at least two experiments.

Microscopy and photography

Scanning electron microscopy was performed as previously described (Garces et al., 2007).

Light and fluorescent microscopy was performed using a Zeiss Discovery V12 stereomicroscope and photographed using an AxioCam MRc digital camera (Carl Zeiss MicroImaging, Thornwood, NY, USA). For fluorescent imaging, the microscope was equipped with an X-Cite 120 light source, a pentafluor GFP wideband cube (Zeiss KSC 295-831D, excitation HQ 470/440 nm and dichroic mirror 495LP) and a long-pass emission filter (KS295-831WD, 500 nm). In addition, specificity of the GFP signal was confirmed using a band-pass filter with the same excitation characteristics (KSC 295-831D 525/550BP). All experiments are representative of at least 20 viewed apices from at least two independent experiments. Other digital photographs were taken with an Olympus SP300UZ camera (Olympus, Green Valley, PA, USA). Images of in situ hybridization and GUS staining experiments were captured using a Nikon Eclipse E600 compound microscope and a Nikon digital camera. Confocal microscopy for SlPIN1 immunolocalization and PIN1:GFP live images was performed as described (Bayer et al., 2009). All photographs were adjusted for brightness and contrast and assembled into figures using Adobe Photoshop 7.0.1 (Adobe Systems, San Jose, CA, USA).

Generation of *ENTIRE* transgenic tomato plants

The *ENTIRE* open reading frame was amplified from tomato cDNA using the primers IAA9-F5 (5′-GGTTCCCACAGGATTATTAGAGTG-3′) and IAA9-R1 (5′-ATAGGCTAATTTCTGCTCCG-3′), and cloned into the pCR8/GW/TOPO vector utilizing the manufacturer's protocol (Invitrogen, Carlsbad, CA, USA) to create the pCR8ENTIRE clone. A Gateway LR cloning reaction was then performed according to the manufacturer's specification to transfer the *ENTIRE* fragment to the binary vector pK2GW7 (Karimi et al., 2002), generating the p35S:*ENTIRE* construct.

The p35S:*ENTIRE*Δ construct was generated by amplifying the *ENTIRE* open reading frame in two parts from the pCR8ENTIRE clone using the primers IAA9-F5 and IAA9mutR (5′-TCTAAAAGATC-GAATGGGTGACCAACCAAC-3′) for the 5′ fragment, and IAA9-R1 and IAA9mutF (5′-GTTGGTTGGTCACCCATTCGATCTTTTAGA-3′) for the 3′ fragment. The combined PCR products were used as a template in an additional PCR reaction using primers IAA9-F5 and IAA9-R1 with the Expand Long Template PCR System (Roche, Basel, Switzerland). This PCR product was cloned and transferred to a binary vector as described above.

Both constructs were introduced into the *A. tumefeciens* strain GV3101, and then transformed in parallel into the tomato cultivar VF36 by the tissue culture method at the Ralph Parsons Plant Transformation Center (University of California Davis).

RT-PCR and qRT-PCR analysis of *ENTIRE* transgenic lines

Duplicate RNA extractions were performed on expanding leaves using the QIAGEN RNeasy Plant Mini Kit (Germantown, MD, USA). All samples were treated using RQ DNAse (Promega) and were ethanol precipitated. cDNA synthesis was performed using the Superscript III First-Strand Synthesis System for RT-PCR (Invitrogen, Carlsbad, CA, USA) with 500 ng RNA and using the oligo(dT) primer. qRT-PCR was performed as previously described (Kimura et al., 2008), using the same control primers for *GAPDH* and using *ENTIRE* gene-specific primers (IAA9q-F1, 5′-GCCTTCTGCTGTGAATGATGC-3′ and IAA9qR1, 5′-TTCCGT-CAACCTCTTCGTTATTCTTCG-3′). For *p35S:ENTIRE*Δ RT-PCR, RNA extraction and cDNA synthesis were carried out similarly. PCR products generated with the IAA9q-F1 and IAA9-R1 primers were digested with *Bst*EII and visualized on 2% agarose gels.

Generation of the *DR5:GUS* transgenic tomato plants

The DR5(7x) promoter fused in-frame to *GUS* in the pUC19 vector was received from T. Guilfoyle (Ulmasov et al., 1995). The DR5(7x) fragment was cloned into the pCR8/GW/TOPO TA entry vector (Invitrogen, Carlsbad, CA, USA) after PCR amplification with primers M13-R and DR5-TATA-R (5′-CATTTGGAGAGGTATTTTACAAC-3′). An LR cloning reaction was performed using the entry vector containing the DR5(7x) fragment and the destination vector pKGWFS7 (Karimi et al., 2002) according to the manufacturer's protocol. Transgenic plants were generated as described above.

GUS staining

Histochemical localization of GUS activity was performed as previously described (Kang and Dengler, 2002). Images are representative of >20 observed samples stained in three independent experiments.

RESULTS

Auxin transport and response in tomato incipient leaflet primordia

First, we determined whether auxin accumulates in the initiating leaflets of transgenic plants harboring the *pDR5:GUS* auxin response reporter. GUS staining in the leaves of these transgenics was faint in P2 leaf tips and subsequently strongly upregulated (Fig. 1A). Leaflet primordia showed a near-identical pattern of GUS expression (Fig. 1B-D). Thus, the response to auxin appears to be activated in a similar manner at the tips of both developing leaves and leaflets. Under our staining conditions, GUS expression was not reliably detected in younger leaf primordia despite previous evidence that the response to auxin is activated in these tissues (Bayer et al., 2009; Reinhardt et al., 2000; Reinhardt et al., 2003). This result suggested that a more sensitive reporter was necessary to visualize the response to auxin in initiating and incipient leaflets.

To this end, we examined the expression of GFP in tomato plants transformed with a pPIN1:PIN1:GFP construct (Bayer et al., 2009; Benkova et al., 2003). The expression of PIN1 is known in several species to be auxin responsive (Bai and DeMason, 2006; Bayer et al., 2009; Gallavotti et al., 2008; Heisler et al., 2005), and GFP localization in tomato plants transformed with this construct is indistinguishable at the shoot apex from endogenous tomato PIN1 localization (Bayer et al., 2009). We further confirmed the auxin responsiveness of the *pPIN1:PIN1:GFP* transgene in tomato leaves by visualizing the induction of GFP expression after the application of exogenous auxin in transformed plants (see Fig. S1 in the supplementary material). The earliest signs of leaflet outgrowth in tomato are visible at the flanks P3 leaf primordia. Subtle, but reproducible, expression of GFP marked the site of the first leaflet in P3 leaf primordia (Fig. 1E,F; white arrowheads). Subsequent leaflet outgrowth coincided with a strong upregulation of GFP expression (Fig. 1G-J, white arrowheads). A similar pattern was seen during the initiation of additional leaflets and lobes (Fig. 1I-K, white and red arrowheads). GFP was low or absent in the regions that give rise to the bladeless intercalary tissue (Fig. 1I, blue arrowheads). PIN1:GFP and DR5:GUS expression indicates that the response to auxin is activated in developing leaflets and lobes during their initiation, and repressed in regions that separate leaflets.

We further examined PIN1:GFP expression in live shoots using confocal microscopy. GFP expression was strongly induced in initiating leaflets relative to the surrounding intercalary regions, confirming our previous results (Fig. 2A, white and blue arrowheads). Induction of GFP could be seen prior to the bulging of the leaflet primordia (Fig. 2A, orange arrowhead). Internal optical sections of developing leaflets revealed a strong basal localization of GFP in the presumptive vascular trace (Fig. 2B), with an apical subcellular localization in epidermal optical sections (Fig. 2C,D). These results suggest that auxin is transported through the epidermis of developing leaflets towards the apex, where it is funneled basally through the presumptive vascular tissues.

Next we examined whether the active transport of auxin, as evidenced by the localization of native tomato PIN1 (referred to here as SlPIN1), determines the site of leaflet initiation in tomato leaves. SlPIN1 was upregulated in leaflets and lobes initiating from the flanks of developing leaves, consistent with the observed PIN1:GFP expression (Fig. 2E-K and for lower magnification see Fig. S2 and Movie 1 in the supplementary material). The examination of SlPIN1 intracellular localization revealed that epidermal convergence points correlated with the predicted site of leaflet and lobe initiation (Fig. 2E,I). After initiation, epidermal SlPIN1 localized towards the apex of both lobes and leaflets (Fig. 2F,J), whereas the internal

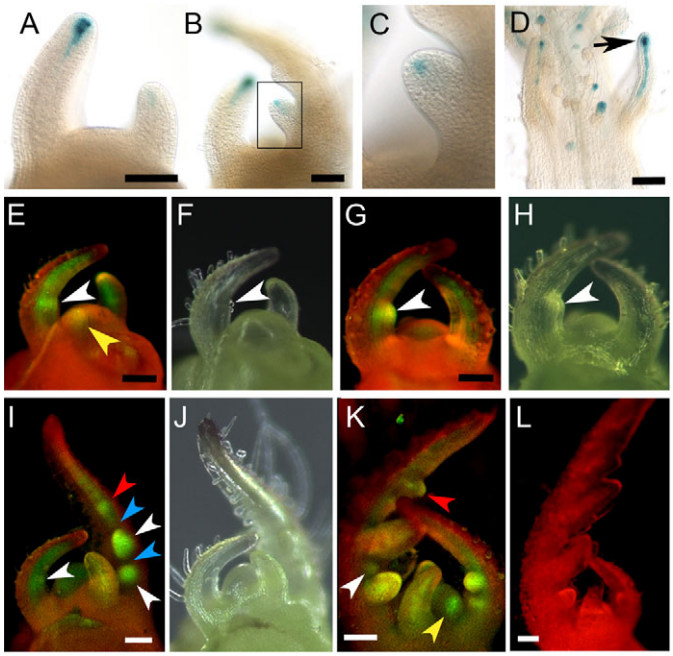

Fig. 1. Auxin response coincides with leaflet initiation. (**A-D**) DR5 expression in young leaves (A) and leaflets (B-D). Boxed leaflet in B is shown at higher magnification in C. Arrow in D shows leaflet tip in an older leaf. (**E**,**G**,**I**,**K**) Fluorescent microscopy of *pPIN1:PIN1:GFP* shoots showing the induction of GFP expression in initiating leaves (yellow arrowheads), leaflets (white arrowheads) and lobes (red arrowheads). Low GFP expression is seen in the regions between leaflets (blue arrowheads). (**F**,**H**,**J**) Light microscopy of shoots corresponding to E, G and I. (**L**) Wild-type plant showing no GFP expression. Scale bars: 100 μm.

localization of SlPIN1 is directed away from the growing leaflet or lobe tip in the provascular tissues (Fig. 2E,I) (Bayer et al., 2009). Cells flanking the predicted site of the leaflet vascular strand showed lateral SlPIN1 localization directed towards the provascular tissue (Fig. 2G). A strong epidermal SlPIN1 polarization away from the bulging first leaflet, and towards the incipient second leaflet, was observed at the leaflet primordia base (Fig. 2H). These results suggest that auxin is transported to the site of leaflet and lobe initiation through the epidermis from which it is drained internally through the provascular tissue. The formation of these convergence points occurs prior to any other observable sign of leaflet specification. This patterning process is reminiscent of that reported during primordia initiation in the SAM (Benkova et al., 2003; Reinhardt et al., 2003).

Inhibition of auxin transport during early leaf development

Several previous studies have suggested that the disruption of auxin transport by chemical inhibitors results in a reduction in leaf complexity (Avasarala et al., 1996; DeMason and Chawla, 2004; Reinhardt et al., 2000; Wang et al., 2005), but the developmental mechanism of this leaf simplification remains unclear. We further examined the effect of disrupting auxin transport in compound leaves by culturing tomato shoot apical meristems on media containing the auxin transport inhibitor N-1-napthylphthalamic acid (NPA) (Fig. 3). We examined the effect of NPA treatment prior to leaflet initiation by culturing shoots dissected to remove all but the

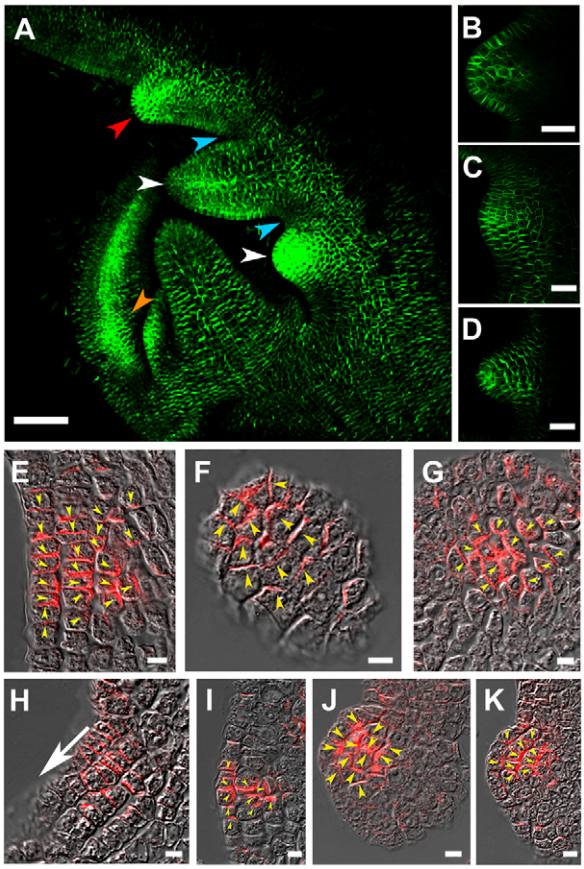

Fig. 2. Auxin is transported to the site of leaflet initiation. (**A**) Live image of *pPIN1:PIN1:GFP* shoot showing incipient (orange arrowhead) and developing (white arrowheads) leaflets, a developing lobe (red arrowhead) and intercalary regions with low GFP expression (blue arrowhead). (**B**) PIN1:GFP is basally localized in the provascular tissues. (**C**) Epidermal convergence of PIN1:GFP in an initiating leaflet. (**D**) Apical epidermal PIN1:GFP in an initiated leaflet. (**E-K**) SlPIN1 immunolocalization (red) in developing leaflets and lobes. Yellow arrowheads indicate the direction of SlPIN1 polarization. (E) SlPIN1 convergence point at an incipient leaflet. (F) Oblique section through the epidermis of a developing leaflet showing apical SlPIN1 localization. (G) Internal section of a developing leaflet showing lateral SlPIN1 localization towards the presumptive site of a vascular strand. (H) Epidermal section at the base of an initiated leaflet showing strong basal SlPIN1 localization (white arrow) towards the site of the next leaflet. (I) SlPIN1 convergence point in an incipient lobe. (J) Section through the epidermis of the tip of a lobe showing convergent SlPIN1 localization. (K) Internal section through the same lobe as in J showing basal localization of SlPIN1 in the developing vascular strand. Scale bars: 100 μm in A, 25 μm in B-D; 5 μm in E-K.

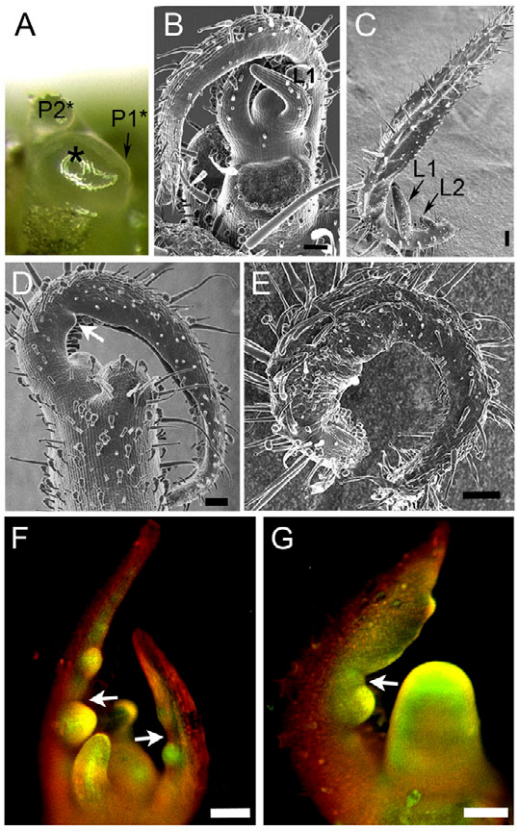

Fig. 3. Auxin transport mediates compound leaf development. (**A**) Example of a dissected meristem, with the remaining leaf primordia indicated (P1* and P2*). The SAM is labeled with an asterisk. (**B**) Control apex with a P1* primordium. (**C**) Control P2* primordium. (**D**) P1* primordium on an NPA-treated apex. Arrow shows a small underdeveloped leaflet. (**E**) An NPA-treated P2* simple leaf. (**F**) PIN1:GFP expression in control media. (**G**) NPA-treated *pPIN1:PIN1:GFP* apex. Arrows in F and G show the expected intercalary region. L marks lateral leaflets numbered corresponding to the order of their initiation. Scale bars: 100 μm.

leaf primordia at stages P1 and P2 (termed P1* and P2* for identification as development progressed; Fig. 3A). P1* and P2* leaves from shoots grown on control media developed in a similar pattern to that of wild-type leaves in whole plants (Fig. 3B,C). All control P1* and P2* leaves had produced at least one pair of lateral leaflets after 7 days of growth on media (see Table S1 in the supplementary material). In P1* leaves, the first pair of lateral leaflets was initiated and was expanding at the time of visualization (Fig. 3B). P2* primordia had initiated one or two pairs of lateral leaflets (Fig. 3C). In comparison to controls, NPA-treated leaves were generally reduced in leaf complexity (Fig. 3D,E; see Fig. S3 in the supplementary material). The range of phenotypic severity included leaves that initiated leaflets resembling those of wild type to leaves lacking clearly defined lateral leaflet primordia (Fig. 3D,E; see Fig. S2 in the supplementary material). Approximately 20% of P2* and 45% of P1* leaf primordia failed to produce lateral leaflet primordia that were separated from the terminal leaflet (see Table S1 in the supplementary material). In addition, blade outgrowth was further advanced in the terminal leaflet of NPA-treated P1* leaves (Fig. 3D) when compared with control P1* leaves (Fig. 3B). In strongly affected NPA-treated P2* leaves, leaflet primordia were absent and were replaced with blade outgrowth (compare Fig. 3C with 3E). A timecourse performed on control and NPA-treated leaves further demonstrated that blade outgrowth was initiated in place of leaflet primordia (see Fig. S4 in the supplementary material). NPA treatment of the *pPIN1:PIN1:GFP* reporter plants showed that the initiation of ectopic blade outgrowth correlated with the activation of GFP expression (Fig. 3F,G, white arrows). A similar activation of the response to auxin after NPA treatment has also been reported in the shoot apical meristem and in developing simple leaves (Heisler et al., 2005; Wenzel et al., 2007). These results demonstrate that auxin transport is important for several stages of

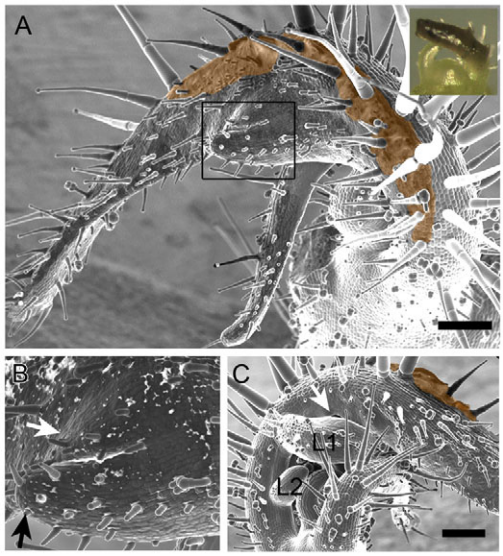

Fig. 4. Ectopic auxin can induce blade outgrowth. (**A**,**B**) Leaf treated with 1 mM IAA showing ectopic blade outgrowth with a fused leaflet structure (box in A outlines region of higher magnification in B). Inset shows a representative application. White arrow in B shows ectopic blade outgrowth and black arrow shows the leaflet-like structure. Orange shading highlights the remaining paste from auxin application. (**C**) The opposite side of the leaf shown in A and B, initiating leaflets in a normal pattern. White arrow shows restricted blade outgrowth in the intercalary region. Scale bars: 100 μm.

compound leaf development. First, NPA treatment negatively influences leaflet development, suggesting that the active accumulation of auxin in presumptive leaflets is important for their initiation, probably in a manner similar to that observed in leaf primordium initiation at the shoot apex (Reinhardt et al., 2000; Reinhardt et al., 2003). Second, the inhibition of auxin transport and subsequent failure to restrict the response to auxin between leaflet primordia results in ectopic laminar outgrowth. This implies that both the accumulation of auxin in leaflet primordia and the complementary lack of auxin in the surrounding tissues is important for establishing the boundaries separating leaflets.

Auxin application to developing leaves

We tested whether auxin gradients are important to designate bladeless and bladed regions of compound leaves by applying auxin to developing leaf primordia. The auxin indole-3-acetic acid (IAA) was mixed with lanolin paste at concentrations that were previously determined to be physiologically relevant (Reinhardt et al., 2000; Reinhardt et al., 2003; Uggla et al., 1996) and applied as a broad band across one side of a P3 leaf primordium. Such applications resulted in blade outgrowth coinciding with the site of application (Fig. 4A and white arrow in Fig. 4B). Outgrowth occurred in 5 of 14 leaves treated with 1 mM IAA and 13 of 14 leaves treated with 10 mM IAA (see Table S2 in the supplementary material). In most cases this outgrowth was asymmetric so that the untreated half of the leaf served as an internal control; it remained compound with restricted blade outgrowth between leaflets in the intercalary regions (Fig. 4C, arrow). Furthermore, lateral leaflet-like structures continuous with the terminal leaflet via ectopic blade outgrowth were still observed on the treated half of some of these leaves (Fig. 4A and black arrow in Fig. 4B). Thus auxin treatment did not exclusively inhibit leaflet initiation, but rather activated blade outgrowth on the rachis (Fig. 4B). Control applications performed in parallel had no effect on leaf development (see Table S2 in the supplementary material). These results demonstrate that auxin is sufficient to promote blade outgrowth in the bladeless intercalary tissues, and imply that auxin gradients are key signals patterning compound leaf development.

Next, we determined whether ectopic auxin application is sufficient to induce leaflet initiation. Application of IAA as a spot to early P3-staged leaves (Fig. 5) resulted in two major outcomes when compared with DMSO-treated leaves (Fig. 5A): induction of ectopic blade outgrowth (1 of 42 applications of 1 mM IAA and 9 of 39 applications of 10 mM IAA; Fig. 5B,C) or ectopic leaflet formation (1 of 42 applications of 1 mM IAA and 7 of 39 applications of 10 mM IAA; Fig. 5D-J; see Table S3 in the supplementary material). Application to the distal regions of the leaf primordia resulted in advanced blade outgrowth (Fig. 5B,C; red arrowhead) or the inappropriate initiation of leaflet primordia in the terminal leaflet region (Fig. 5D,E; white arrowhead). Basal applications resulted in the initiation of ectopic leaflet primordia directly adjacent to endogenous primordia, producing a fused structure with at least two distinguishable primordia tips and independent vascular traces (Fig. 5F-J, white arrowheads). An additional group of IAA-treated leaves initiated leaflets that were slightly broader than normal, but did not appear to result from the fusion between two adjacent leaflets (see Table S3 in the supplementary material). Application of DMSO control lanolin paste did not affect leaf development regardless of the application site or size (see Table S3 in the supplementary material). Prolonged growth of treated leaves confirmed the identity of both ectopic leaflets and blades (Fig. 5K-N). Combined, these results demonstrate that auxin is sufficient to induce leaflet initiation, much as it is sufficient to induce leaf initiation at the shoot apex (Reinhardt et al., 2003). In our experiments, auxin could induce both leaflet and blade outgrowth, depending in part on the size of the domain of auxin application (Figs 4 and 5). Thus, restricted peaks of endogenous auxin in untreated tomato leaves or in the exogenous 'spot' application experiments result in leaflet initiation, but diffuse or broad auxin distribution, as in NPA-treated leaves or in the experiments with broad application, result in blade outgrowth and simple leaf development.

The function of *ENTIRE* during tomato leaf development

The classical tomato mutant *entire* develops large simple leaves (Fig. 6A,B). Recent work has revealed that the *entire* phenotype results from loss-of-function mutations in a member of the AUX/IAA gene family (Wang et al., 2005; Zhang et al., 2007). AUX/IAA proteins function as repressors of the response to auxin by binding and inhibiting the AUXIN RESPONSE FACTOR family of transcription factors, which mediate the auxin transcriptional response (Quint and Gray, 2006). The presence of auxin results in AUX/IAA degradation and activation of the response to auxin. We therefore hypothesized that *ENTIRE* represses the response to auxin in leaves, and that the large simple leaf phenotype of *entire* mutants results from the ectopic or constitutive activation of auxin response pathways.

To determine the nature of leaf simplification in *entire*, we examined early leaf development in the mutant and in wild type. As previously reported, *entire* leaves resembled wild type during early development (Fig. 6C,D), but initiated leaflets later and in reduced number as compared with wild-type leaves (Dengler, 1984). Nevertheless, most *entire* leaves initiated at least two pairs of lateral leaflets that elongated in a similar fashion to wild-type

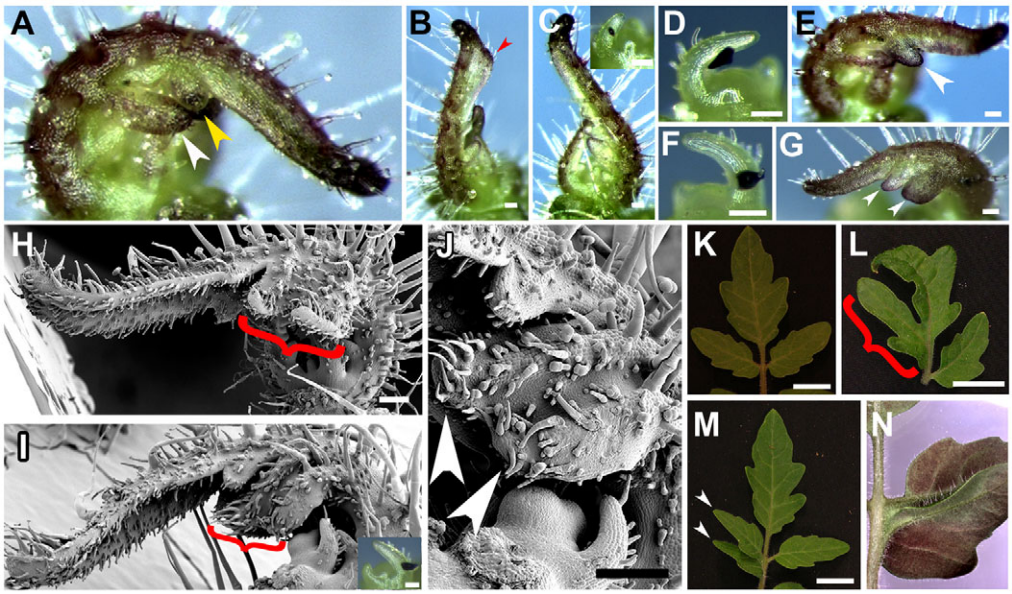

Fig. 5. Auxin induces leaflet initiation. (**A**) A DMSO-treated leaf initiating the first leaflet (white arrowhead) and the first lobe (yellow arrowhead) of the terminal leaflet. (**B-J**) IAA-treated leaves. Leaf primordia are shown directly after application (C inset,D,F,I inset) and after several days of growth (B,C,E,G-J). (B,C) Increased blade outgrowth resulting from distal application of 10 mM IAA (red arrowhead). (D,E) An ectopic leaflet primordium is initiated in the terminal leaflet region associated with the 1 mM auxin treatment site (white arrowhead). (F-H) 10 mM IAA application to the base of a developing leaf (F) induces ectopic fused leaflets (G, arrowheads), which are joined to the terminal leaflet by subsequent blade outgrowth (H, red bracket). (I,J) 10 mM IAA application to the leaf base resulting in an ectopic fused leaflet independent from the terminal leaflet (red bracket in I, higher magnification in J). Arrowheads in J indicate the leaflet tips. (**K-N**) Phenotypes of treated leaves after prolonged growth. (K) DMSO-treated leaf. (L-N) 10 mM IAA-treated leaves with ectopic blade (L, red bracket) and with ectopic leaflets (M, white arrowheads). (N) Abaxial side of the leaf from M showing the independent vascular traces and blades of the two adjacent leaflets. Scale bars: 100 μm in A-J; 1 cm in K-M.

leaflets (Fig. 6E-H). In wild-type plants, outgrowth is restricted at the base of the terminal leaflet, clearly separating the lateral leaflets from the terminal leaflet (Fig. 6E,G; arrows). In contrast to wild type, *entire* leaves failed to inhibit blade outgrowth at the base of the terminal leaflet, resulting in a fusion between the terminal and lateral leaflets (Fig. 6F,H; arrows). We examined whether this ectopic blade was associated with an activation of the response to auxin by crossing the *pPIN1:PIN1:GFP* transgene into the *entire* mutant background. The *entire* mutation resulted in the diffuse activation of GFP expression in the intercalary regions between the terminal leaflet and the lateral leaflets (Fig. 6I). These results suggest that *ENTIRE* functions by inhibiting the response to auxin between initiating leaflets. Loss of *ENTIRE* function results in ectopic activation of the response to auxin in these regions, leading to the initiation of blade outgrowth.

mRNA localization of *ENTIRE* during tomato leaf development

ENTIRE mRNA expression was evident in the SAM itself, as well as in the developing vascular traces just below the SAM (Fig. 7A-D). In leaves, expression was observed in the provascular trace and throughout the leaf margins at the P3 stage of development (Fig. 7A-C), with the base of the margin showing more intense staining (Fig. 7B,D). *ENTIRE* expression was evident even subsequent to leaflet initiation (Fig. 7D,G,H), but was downregulated at the margin as the blade expanded in older tissues (Fig. 7E,F). *ENTIRE* expression is clearly maintained in the subepidermal tissues of the leaf margins that will give rise to both blade and rachis regions of the leaf (Fig. 7H). In summary, *ENTIRE* mRNA is broadly associated with the marginal blastozone and vascular tissues in developing leaves. *ENTIRE* mRNA was detected throughout the margin, despite its role in defining bladeless rachis regions. This result, in combination with the observation that *ENTIRE* overexpression results in no change in leaf phenotype (Wang et al., 2005), suggests that *ENTIRE* function might be regulated post-transcriptionally.

Expression of auxin-resistant ENTIRE in transgenic tomato

An obvious candidate for the regulation of ENTIRE is auxin itself. We hypothesized that auxin patterns ENTIRE activity at the protein level through degradation, and that this degradation is sufficient to establish normal patterns of blade outgrowth, even in transgenic plants overexpressing the *ENTIRE* transcript. We tested this hypothesis by comparing the phenotypes of plants transformed with either the wild-type *ENTIRE* coding region (referred to here as *ENTIRE*) or a mutated version of *ENTIRE* (referred to here as *ENTIREΔ*) carrying a single amino acid substitution (see Fig. S5 in the supplementary material), known to confer auxin resistance in two other AUX/IAA genes (Dreher et al., 2006; Nagpal et al., 2000; Tian and Reed, 1999). Both versions were cloned with the 35S promoter to confer ubiquitous expression .

p35S:ENTIRE transgenics fell into two categories. The first group of transgenics (4 of 13 lines) could not be differentiated from wild type, as reported previously (Fig. 8A,B). The second group (9 of 13 lines) showed varying intensities of the *entire* phenotype, suggesting downregulation of the *ENTIRE* transcript via cosuppression (Fig. 8C). qRT-PCR showed that the *ENTIRE* transcript level correlated

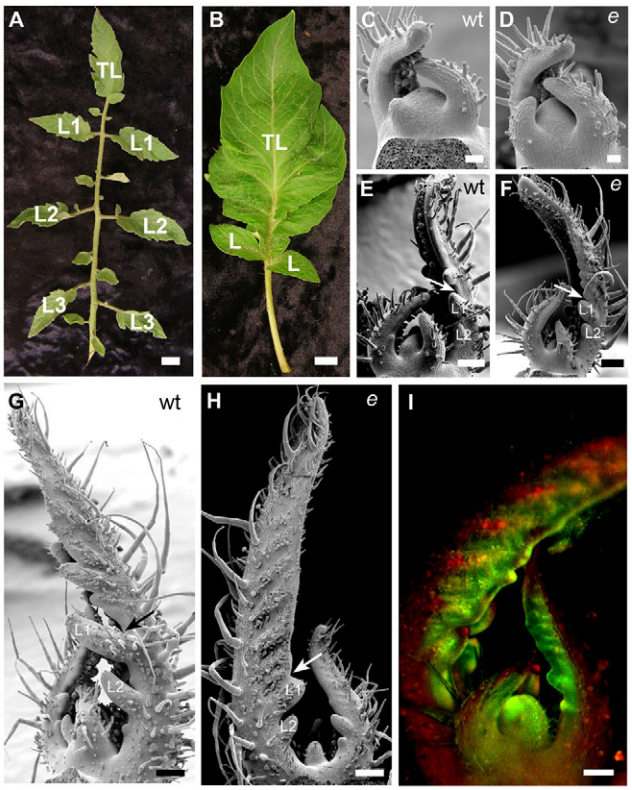

Fig. 6. *ENTIRE* inhibits blade outgrowth in the absence of auxin. (**A**) A wild-type tomato leaf. (**B**) Near-simple leaves of the *entire* mutant. (**C-H**) Leaf development in wild-type (C,E,G) and *entire* (D,F,H) leaves. Arrows in E-H indicate intercalary region in wild type and ectopic blade in *entire* leaves. (**I**) PIN1:GFP expression in *entire*. TL, terminal leaflet; L, lateral leaflets. Scale bars: 1 cm in A,B; 50 μm in C,D; 100 μm in E-I.

with the phenotype (see Fig. S6 in the supplementary material). These data are consistent with previous work that suggested that overexpression of the *ENTIRE* transcript does not result in novel phenotypes (Wang et al., 2005).

By contrast, *p35S:ENTIREΔ* transgenics showed a novel phenotype (6 of 11 transgenic lines). These plants were strongly dwarfed as a result of inhibited internode elongation (Fig. 8D), and in two cases terminated apical growth by producing a pin-like structure (Fig. 8E,F). These phenotypes are similar to those described for *A. thaliana* AUX/IAA gain-of-function mutants that result in auxin insensitivity (Hamann et al., 2002; Hamann et al., 1999; Leyser et al., 1996). The leaves produced from these plants showed strongly restricted lateral outgrowth (Fig. 8G-I). Blade outgrowth was inhibited, resulting in narrow leaflet blades that curled abaxially (Fig. 8G). Leaflet production was also inhibited, frequently resulting in unipinnate trifoliate leaves (Fig. 8H). In addition to these novel phenotypes, both wild-type (2 of 11 lines) and *entire*-like (3 of 11 lines) phenotypes were observed. In one line, chimeric leaves with features of both the *entire* loss-of-function and *p35S:ENTIREΔ* gain-of-function phenotypes were produced (Fig. 7I). The expression of the mutated transcript could be visualized in lines with novel phenotypes using a restriction polymorphism between the wild-type and mutated sequences (see Fig. S6 in the supplementary material). Together, these results suggest that auxin-mediated degradation of ENTIRE specifies appropriate lateral growth during early leaf development.

The role of *IAA8* and *IAA9* in *A. thaliana* simple leaves

Previous studies have shown that auxin and auxin transport may designate initiating serrations in *A. thaliana* simple leaf development (Hay et al., 2006). *ENTIRE* belongs to the subfamily IV clade of AUX/IAA genes (Wang et al., 2005). The *A. thaliana* genome contains two genes, *IAA8* and *IAA9*, that belong to this clade. The Columbia (Col) ecotype of *A. thaliana* produces leaves with marginal serrations (Fig. 9A). Leaves of both *iaa9-1* and *iaa8-1* single mutants were indistinguishable from wild type (Fig. 9B,C), but *iaa8 iaa9* double mutants produced leaves with completely entire margins (Fig. 9D). Examination of early leaf development in Col and *iaa8 iaa9* plants revealed that serrations were still initiated in the double mutant but, as the leaf developed, restriction of blade outgrowth was not maintained in the developing sinuses (Fig. 9E-J). These results demonstrate that

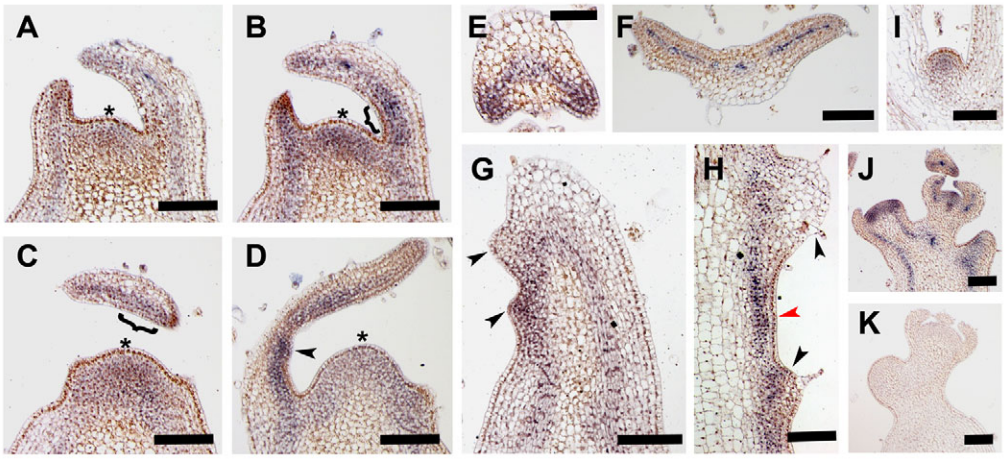

Fig. 7. *ENTIRE* mRNA localization during leaf development. (**A-C**) Serial sections through a SAM with a P3 primordium (right) before leaflet initiation, showing vascular (A) and marginal (B,C) expression. (**D**) Expression in the margin of a leaf just after the initiation of the first leaflet. (**E**,**F**) Transverse section through young (E) and older (F) leaves. (**G**) Staining in the second primary leaflet during initiation. (**H**) Subepidermal expression of *ENTIRE* in both the rachis and initiating leaflet tissues. (**I**,**J**) *ENTIRE* transcript could also be detected in other meristematic tissues such as lateral buds (I) and floral meristems (J). (**K**) Sense control for *ENTIRE*. SAMs (*),initiating leaflets (black arrowheads), rachis (red arrowheads) and marginal tissues (brackets) are marked. Scale bars: 100 μm for A-D,F,G,I-K; 50 μm for E,H.

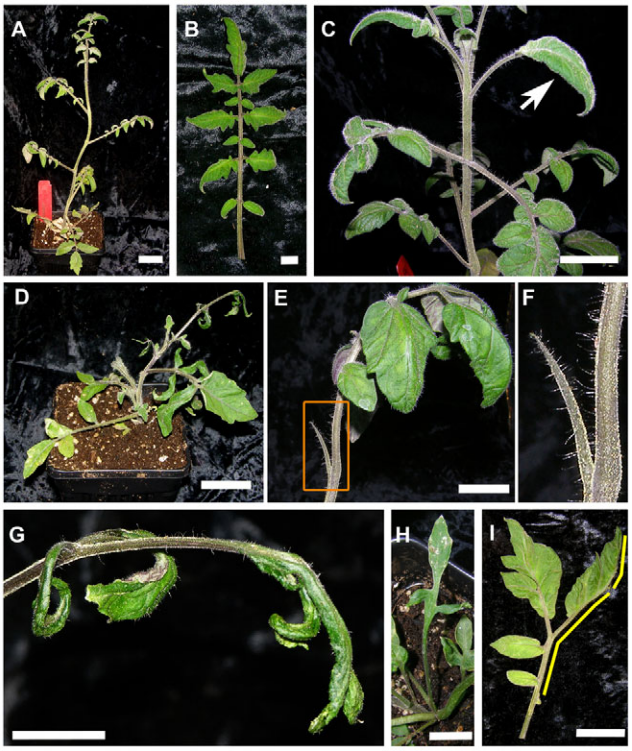

Fig. 8. *ENTIRE* inhibits lateral growth in leaves. (**A-C**) *p35S:ENTIRE* transgenics. Wild-type phenotype in plant stature (A) and leaf shape (B). (C) Another *p35S:ENTIRE* transgenic line showing *entire*-like phenotype (arrow). (**D-I**) *p35S:ENTIREΔ* transgenic phenotypes included reduced plant stature (D) and shoot termination in a pin-like structure (E,F; boxed area in E is shown at higher magnification in F). Lateral growth in these plants was reduced resulting in a reduced blade (G) and the production of trifoliate leaves (H). (I) A transgenic line showing partial inhibition of leaflet and blade outgrowth (yellow line indicates region lacking blade and leaflet initiation). Scale bars: 5 cm in A,C,D; 2 cm in B,G,I; 2.5 cm in E; 1 cm in H.

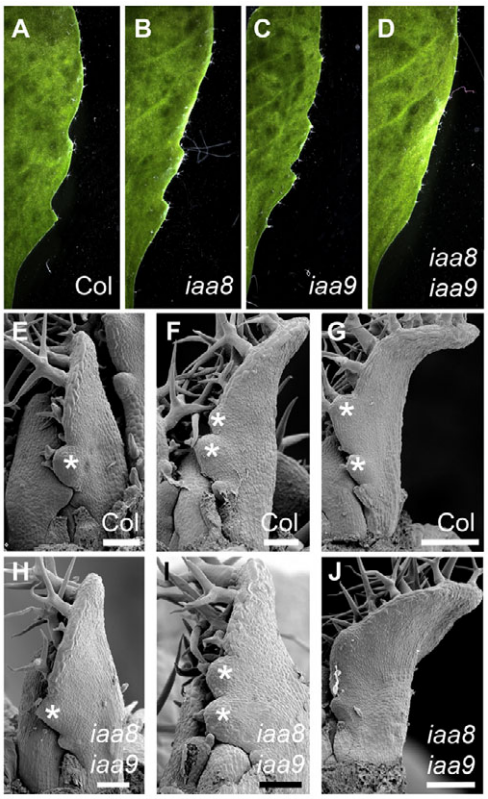

Fig. 9. *IAA8* and *IAA9* regulate *A. thaliana* serration development. (**A-C**) Columbia (*A. thaliana* ecotype, A), *iaa8-1* (B) and *iaa9-1* (C) leaf edges with serrations and (**D**) *iaa8-1 iaa9-1* double mutant leaf lacking serrations. (**E-J**) Serration development in Col (E-G) and *iaa8 iaa9* mutant (H-J) leaves. Asterisks mark serrations. Scale bars: 100 μm.

IAA8 and *IAA9* redundantly reduce blade outgrowth between developing serrations, resembling the role of *ENTIRE* in restricting blade outgrowth between developing leaflets.

DISCUSSION

Compound leaf development is separated into two main stages; primary morphogenesis, in which leaflet primordia are initiated, and secondary morphogenesis, in which regulated blade outgrowth delineates the independence of mature leaflets (Bharathan et al., 2002; Dengler and Tsukaya, 2001). Our experiments show that the plant hormone auxin patterns leaf development during both of these stages. These experiments suggest a simple model by which leaf dissection might be achieved through the opposing activities of auxin and *ENTIRE*.

Auxin promotes the initiation of leaflets

The first major morphogenic event in compound leaf development is the initiation of leaflet primordia during primary morphogenesis. Until recently, very little was known about the specification of leaflet initiation. Studies in pea, *C. hirsuta* and tomato have implicated auxin transport in leaflet initiation (Avasarala et al., 1996; Barkoulas et al., 2008; DeMason and Chawla, 2004; Reinhardt et al., 2000), and work in *C. hirsuta* revealed the upregulation of the response to auxin in incipient leaflet primordia (Barkoulas et al., 2008). We find that activation of the response to auxin also occurs in tomato incipient leaflets. Moreover, we show that leaflet initiation events are predicted by the formation of SlPIN1 convergence points in the leaf epidermis. Inhibition of auxin transport in tomato apices reproduced the previously reported simplified leaf phenotype (Avasarala et al., 1996), and our developmental analysis confirmed that this simplification occurred in part by the inhibition of leaflet initiation. Finally, auxin is sufficient to induce the outgrowth of ectopic leaflet primordia when applied to developing tomato leaves. Together, these results demonstrate a role for PIN-driven auxin gradients during leaflet initiation. This mechanism of leaflet initiation is evolutionarily conserved despite the independent derivation of the compound leaf trait in these species.

The role of auxin in secondary morphogenesis

Unlike that of leaflet initiation, the molecular regulation of fractionated blade outgrowth during secondary morphogenesis remains a complete mystery. Exogenous application of auxin to the entire *C. hirsuta* shoot resulted in ectopic blade initiation in some leaves, but it is unclear how direct this effect was on developing leaves (Barkoulas et al., 2008). We find that treatment of developing tomato leaves with either exogenous auxin (or auxin transport inhibitor to shoots) results in the ectopic initiation of blade outgrowth along the tomato leaf rachis. This demonstrates that the rachis is

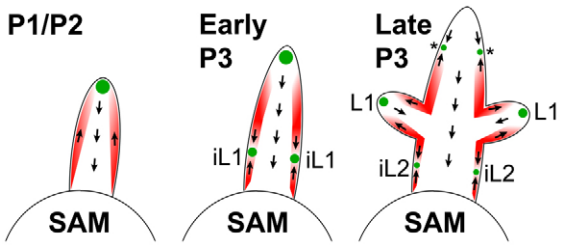

Fig. 10. Model of the regulation of compound leaf development by auxin and the response to auxin. Auxin maxima (green spots), direction of auxin flow (arrows), hypothetical *ENTIRE* activity (red bands), leaflets (L), incipient leaflets (iL) and incipient lobes (*) are indicated.

competent for blade expansion, but is prevented from doing so by the drainage of auxin into the adjacent incipient leaflets. Therefore, the pattern of auxin distribution that promotes the initiation of leaflet primordia during primary morphogenesis also informs on the pattern of blade outgrowth during secondary morphogenesis.

The role of *ENTIRE* during tomato compound leaf development

The bladeless identity of rachis tissues is maintained through the activity of the AUX/IAA gene *ENTIRE*, as evidenced by the ectopic initiation of blade outgrowth and the response to auxin along the rachis in the *entire* loss-of-function mutant. Ultimately, *entire* leaves are simple or near-simple despite the presence of leaflet primordia during primary morphogenesis. This phenomenon is reminiscent of many naturally occurring simple-leafed species that also initiate leaflet primordia during early development (Bharathan et al., 2002). Despite the role of *ENTIRE* in marginal dissection, *ENTIRE* mRNA was found throughout the leaf margin. The expression of an auxin-resistant form of ENTIRE results in inhibited marginal growth in leaves, whereas the expression of a wild-type version does not, implying that auxin-mediated degradation of ENTIRE is important to allow the specification of lateral growth in leaves. Together, these results suggest that *ENTIRE* and auxin act in opposition to specify differential growth during tomato compound leaf development. It is tempting to speculate that the accumulation of auxin at the incipient leaflet and the subsequent degradation of ENTIRE causes leaflet outgrowth. Correspondingly, auxin is drained into leaflets from adjacent rachis tissues, thus preventing ENTIRE degradation and inhibiting outgrowth in the rachis (Fig. 10). Ultimate proof of this hypothesis awaits the visualization of ENTIRE during leaf development, a difficult task given the rapid turnover of AUX/IAA proteins (Dreher et al., 2006).

Although ENTIRE plays a major role in repressing blade outgrowth, *entire* plants show defects in leaflet initiation as well. This defect could result from feedback between the response to auxin and auxin transport during leaf development. The expression of PIN1:GFP is less refined in the *entire* background, and misregulation of SlPIN1 might prevent the formation of the auxin peaks necessary to specify leaflets. Thus, both negative and positive factors might reinforce the formation of constricted auxin peaks to specify leaflet initiation.

Several other simplified leaf mutants have been molecularly identified in tomato. The simple-leafed *Lanceolate* mutant and the unlobed *procera* mutant reduce the morphogenic capacity of leaves, but have not yet been directly implicated in patterning growth (Jasinski et al., 2008; Ori et al., 2007). By contrast, both *ENTIRE* and *GOBLET* seem to regulate morphogenetic patterning (Berger et al., 2009; Blein et al., 2008; Brand et al., 2007). *GOB* specifies intercalary regions between leaflets in a manner similar to that described here for *ENTIRE,* and *gob* mutant leaves phenocopy *entire* leaves. Unlike *ENTIRE*, *GOB* transcript is expressed specifically in intercalary regions (Berger et al., 2009; Blein et al., 2008). This expression is not dependent on *ENTIRE* function, suggesting that the two genes may act in independent pathways (Berger et al., 2009). The precise definition of the relationship between *ENTIRE*, *GOB* and auxin remains a major question in the current model for tomato leaf dissection.

The homology of simple and compound leaves

Discussion of the homology between simple and compound leaf types dates at least to the eighteenth century writings of Johann Goethe, and is centered around two major interpretations (Arber, 1950; Champagne and Sinha, 2004). The first hypothesis suggests that simple, lobed and compound leaves represent a continuum in which unequal blade outgrowth gives rise to increasingly defined marginal protrusions (Kaplan, 1975). Under this theory, the leaf is generally considered to be a discrete unit relative to the shoot. The competing hypothesis argues that compound leaf primordia are shoot-like, and leaflets initiate in a process homologous to leaf initiation at the shoot apical meristem (Sattler and Rutishauser, 1992). The question of the homology of shoots and leaves has important evolutionary and developmental implications, and has thus received renewed interest in the era of modern molecular biology.

A significant amount of data has now accumulated suggesting that the molecular regulation of compound leaf development involves processes similar to those regulating shoot development. These include regulation by KNOX genes and patterning via the auxin/PIN developmental module (Barkoulas et al., 2008; Bharathan et al., 2002; Hay and Tsiantis, 2006). Despite these findings, our results and those of others have begun to uncover a conserved molecular network regulating marginal dissection in both simple and compound leaves, which includes *ENTIRE* and its orthologs, PIN1, auxin and NAM/CUC orthologs (Barkoulas et al., 2008; Berger et al., 2009; Blein et al., 2008; Hay et al., 2006). Perhaps the acquisition of a shoot-like identity promotes leaf dissection by utilizing the existing marginal dissection components, thus combining the heretofore mutually exclusive hypotheses of compound leaf morphogenesis. It also remains to be seen whether other independent origins of compound leaf development utilize similar mechanisms to accomplish the dissected leaf form. Regardless, it is clear that auxin and the response to auxin play a major role in determining leaf shape by modifying growth across the leaf.

Acknowledgements

We thank Drs Julin Maloof, John Harada, Helena Garcês, Rakefet David-Schwartz, Julie Kang and Seisuke Kimura for critical reading of this manuscript, and Kumitaa Theva Das for plant care and technical assistance. We also thank the TGRC, University of California, Davis for tomato stocks, and the Ralph Parsons Transformation Facility for generating transgenic plants. This work was supported by the NSF Developmental Mechanisms Awards 0344743 and 0641696 (to N.S.) and an Elsie Taylor Stocking Memorial Fellowship (to D.K.).

Supplementary material

Supplementary material for this article is available at
http://dev.biologists.org/cgi/content/full/136/17/2997/DC1

References

Arber, A. (1950). *The Natural Philosophy of Plant Form*. Cambridge: Cambridge University Press.

Avasarala, S., Yang, J. and Caruso, J. L. (1996). Production of phenocopies of the lanceolate mutant in tomato using polar auxin transport inhibitors. *J. Exp. Bot.* **47**, 709-712.

Bai, F. and DeMason, D. A. (2006). Hormone interactions and regulation of Unifoliata, PsPK2, PsPIN1 and LE gene expression in pea (Pisum sativum) shoot tips. *Plant Cell Physiol.* **47**, 935-948.
Barkoulas, M., Hay, A., Kougioumoutzi, E. and Tsiantis, M. (2008). A developmental framework for dissected leaf formation in the Arabidopsis relative Cardamine hirsuta. *Nat. Genet*. **40**, 1136-1141.
Bayer, E. M., Smith, R. S., Mandel, T., Nakayama, N., Sauer, M., Prusinkiewicz, P. and Kuhlemeier, C. (2009). Integration of transport-based models for phyllotaxis and midvein formation. *Genes Dev.* **23**, 373-384.
Benkova, E., Michniewicz, M., Sauer, M., Teichmann, T., Seifertova, D., Jurgens, G. and Friml, J. (2003). Local, efflux-dependent auxin gradients as a common module for plant organ formation. *Cell* **115**, 591-602.
Berger, Y., Harpaz-Saad, S., Brand, A., Melnik, H., Sirding, N., Alvarez, J. P., Zinder, M., Samach, A., Eshed, Y. and Ori, N. (2009). The NAC-domain transcription factor GOBLET specifies leaflet boundaries in compound tomato leaves. *Development* **136**, 823-832.
Bharathan, G., Goliber, T. E., Moore, C., Kessler, S., Pham, T. and Sinha, N. R. (2002). Homologies in leaf form inferred from KNOXI gene expression during development. *Science* **296**, 1858-1860.
Blein, T., Pulido, A., Vialette-Guiraud, A., Nikovics, K., Morin, H., Hay, A., Johansen, I. E., Tsiantis, M. and Laufs, P. (2008). A conserved molecular framework for compound leaf development. *Science* **322**, 1835-1839.
Brand, A., Shirding, N., Shleizer, S. and Ori, N. (2007). Meristem maintenance and compound-leaf patterning utilize common genetic mechanisms in tomato. *Planta* **226**, 941-951.
Champagne, C. and Sinha, N. (2004). Compound leaves: equal to the sum of their parts? *Development* **131**, 4401-4412.
DeMason, D. A. and Chawla, R. (2004). Roles for auxin during morphogenesis of the compound leaves of pea (Pisum sativum). *Planta* **218**, 435-448.
DeMason, D. A. and Polowick, P. L. (2009). Patterns of Dr5::Gus expression in organs of pea (Pisum Sativum). *Int. J. Plant Sci.* **170**, 1-11.
Dengler, N. G. (1984). Comparison of leaf development in normal (+/+), *entire* (*e*/*e*), and *Lanceolate* (*La*/+) plants of tomato, *Lycopersicon esculentum* 'Ailsa Craig'. *Bot. Gaz.* **145**, 66-77.
Dengler, N. G. and Tsukaya, H. (2001). Leaf morphogenesis in dicotyledons: current issues. *Int. J. Plant Sci.* **162**, 459-464.
Dreher, K. A., Brown, J., Saw, R. E. and Callis, J. (2006). The Arabidopsis Aux/IAA protein family has diversified in degradation and auxin responsiveness. *Plant Cell* **18**, 699-714.
Fleming, A. J., Caderas, D., Wehrli, E., McQueen-Mason, S. and Kuhlemeier, C. (1999). Analysis of expansin-induced morphogenesis on the apical meristem of tomato. *Planta* **208**, 166-174.
Gallavotti, A., Yang, Y., Schmidt, R. J. and Jackson, D. (2008). The relationship between auxin transport and maize branching. *Plant Physiol.* **147**, 1913-1923.
Galweiler, L., Guan, C., Muller, A., Wisman, E., Mendgen, K., Yephremov, A. and Palme, K. (1998). Regulation of polar auxin transport by AtPIN1 in Arabidopsis vascular tissue. *Science* **282**, 2226-2230.
Garces, H. M., Champagne, C. E., Townsley, B. T., Park, S., Malho, R., Pedroso, M. C., Harada, J. J. and Sinha, N. R. (2007). Evolution of asexual reproduction in leaves of the genus Kalanchoe. *Proc. Natl. Acad. Sci. USA* **104**, 15578-15583.
Hagemann, W. and Glesissberg, S. (1996). Organogenetic capacity of leaves: the significance of marginal blastozones in angiosperms. *Plant Syst. Evol.* **199**, 121-152.
Hamann, T., Mayer, U. and Jurgens, G. (1999). The auxin-insensitive bodenlos mutation affects primary root formation and apical-basal patterning in the Arabidopsis embryo. *Development* **126**, 1387-1395.
Hamann, T., Benkova, E., Baurle, I., Kientz, M. and Jurgens, G. (2002). The Arabidopsis BODENLOS gene encodes an auxin response protein inhibiting MONOPTEROS-mediated embryo patterning. *Genes Dev.* **16**, 1610-1615.
Hay, A. and Tsiantis, M. (2006). The genetic basis for differences in leaf form between Arabidopsis thaliana and its wild relative Cardamine hirsuta. *Nat. Genet.* **38**, 942-947.
Hay, A., Barkoulas, M. and Tsiantis, M. (2006). ASYMMETRIC LEAVES1 and auxin activities converge to repress BREVIPEDICELLUS expression and promote leaf development in Arabidopsis. *Development* **133**, 3955-3961.
Heisler, M. G., Ohno, C., Das, P., Sieber, P., Reddy, G. V., Long, J. A. and Meyerowitz, E. M. (2005). Patterns of auxin transport and gene expression during primordium development revealed by live imaging of the Arabidopsis inflorescence meristem. *Curr. Biol.* **15**, 1899-1911.
Jasinski, S., Tattersall, A., Piazza, P., Hay, A., Martinez-Garcia, J. F., Schmitz, G., Theres, K., McCormick, S. and Tsiantis, M. (2008). PROCERA encodes a DELLA protein that mediates control of dissected leaf form in tomato. *Plant J.* **56**, 603-612.
Kang, J. and Dengler, N. (2002). Cell cycling frequency and expression of the homeobox gene ATHB-8 during leaf vein development in Arabidopsis. *Planta* **216**, 212-219.
Kaplan, D. R. (1975). Comparative developmental evaluation of the morphology of Unifacial leaves in the monocotyledons. *Bot. Jahrb. Syst.* **95**, 1-105.
Karimi, M., Inze, D. and Depicker, A. (2002). GATEWAY((TM)) vectors for Agrobacterium-mediated plant transformation. *Trends Plant Sci.* **7**, 193-195.
Kimura, S., Koenig, D., Kang, J., Yoong, F. Y. and Sinha, N. (2008). Natural variation in leaf morphology results from mutation of a novel KNOX gene. *Curr. Biol.* **18**, 672-677.
Koizumi, K., Naramoto, S., Sawa, S., Yahara, N., Ueda, T., Nakano, A., Sugiyama, M. and Fukuda, H. (2005). VAN3 ARF-GAP-mediated vesicle transport is involved in leaf vascular network formation. *Development* **132**, 1699-1711.
Leyser, H. M. O., Pickett, F. B., Dharmasiri, S. and Estelle, M. (1996). Mutations in the AXR3 gene of Arabidopsis result in altered auxin response including ectopic expression from the SAUR-AC1 promoter. *Plant J.* **10**, 403-413.
Long, J. A., Moan, E. I., Medford, J. I. and Barton, M. K. (1996). A member of the KNOTTED class of homeodomain proteins encoded by the STM gene of Arabidopsis. *Nature* **379**, 66-69.
Mattsson, J., Sung, Z. R. and Berleth, T. (1999). Responses of plant vascular systems to auxin transport inhibition. *Development* **126**, 2979-2991.
Nagpal, P., Walker, L. M., Young, J. C., Sonawala, A., Timpte, C., Estelle, M. and Reed, J. W. (2000). AXR2 encodes a member of the Aux/IAA protein family. *Plant Physiol.* **123**, 563-573.
Okada, K., Ueda, J., Komaki, M. K., Bell, C. J. and Shimura, Y. (1991). Requirement of the auxin polar transport system in early stages of arabidopsis floral bud formation. *Plant Cell* **3**, 677-684.
Ori, N., Cohen, A. R., Etzioni, A., Brand, A., Yanai, O., Shleizer, S., Menda, N., Amsellem, Z., Efroni, I., Pekker, I. et al. (2007). Regulation of LANCEOLATE by miR319 is required for compound-leaf development in tomato. *Nat. Genet.* **39**, 787-791.
Petrasek, J., Mravec, J., Bouchard, R., Blakeslee, J. J., Abas, M., Seifertova, D., Wisniewska, J., Tadele, Z., Kubes, M., Covanova, M. et al. (2006). PIN proteins perform a rate-limiting function in cellular auxin efflux. *Science* **312**, 914-918.
Quint, M. and Gray, W. M. (2006). Auxin signaling. *Curr. Opin. Plant Biol.* **9**, 448-453.
Reinhardt, D., Mandel, T. and Kuhlemeier, C. (2000). Auxin regulates the initiation and radial position of plant lateral organs. *Plant Cell* **12**, 507-518.
Reinhardt, D., Pesce, E. R., Stieger, P., Mandel, T., Baltensperger, K., Bennett, M., Traas, J., Friml, J. and Kuhlemeier, C. (2003). Regulation of phyllotaxis by polar auxin transport. *Nature* **426**, 255-260.
Sattler, R. and Rutishauser, R. (1992). Partial homology of pinnate leaves and shoots: orientation of leaflet inception. *Bot. Jahrb. Syst.* **114**, 61-79.
Scarpella, E., Marcos, D., Friml, J. and Berleth, T. (2006). Control of leaf vascular patterning by polar auxin transport. *Genes Dev.* **20**, 1015-1027.
Tian, Q. and Reed, J. W. (1999). Control of auxin-regulated root development by the Arabidopsis thaliana SHY2/IAA3 gene. *Development* **126**, 711-721.
Uggla, C., Moritz, T., Sandberg, G. and Sundberg, B. (1996). Auxin as a positional signal in pattern formation in plants. *Proc. Natl. Acad. Sci. USA* **93**, 9282-9286.
Ulmasov, T., Liu, Z. B., Hagen, G. and Guilfoyle, T. J. (1995). Composite structure of auxin response elements. *Plant Cell* **7**, 1611-1623.
Vollbrecht, E., Veit, B., Sinha, N. and Hake, S. (1990). The developmental gene *Knotted-1* is a member of a maize homeobox gene family. *Nature* **350**, 241-243.
Vollbrecht, E., Reiser, L. and Hake, S. (2000). Shoot meristem size is dependent on inbred background and presence of the maize homeobox gene, *knotted1*. *Development* **127**, 3161-3172.
Wang, H., Jones, B., Li, Z., Frasse, P., Delalande, C., Regad, F., Chaabouni, S., Latche, A., Pech, J. C. and Bouzayen, M. (2005). The tomato Aux/IAA transcription factor IAA9 is involved in fruit development and leaf morphogenesis. *Plant Cell* **17**, 2676-2692.
Wenzel, C. L., Schuetz, M., Yu, Q. and Mattsson, J. (2007). Dynamics of MONOPTEROS and PIN-FORMED1 expression during leaf vein pattern formation in Arabidopsis thaliana. *Plant J.* **49**, 387-398.
Zhang, J., Chen, R., Xiao, J., Qian, C., Wang, T., Li, H., Ouyang, B. and Ye, Z. (2007). A single-base deletion mutation in SlIAA9 gene causes tomato (Solanum lycopersicum) entire mutant. *J. Plant Res.* **120**, 671-678.